Mobile Emitter Geolocation and Tracking Using TDOA and FDOA Measurements

Darko Mušicki, *Member, IEEE*, Regina Kaune, and Wolfgang Koch, *Senior Member, IEEE*

***Abstract*—This paper considers recursive tracking of one mobile emitter using a sequence of time difference of arrival (TDOA) and frequency difference of arrival (FDOA) measurement pairs obtained by one pair of sensors. We consider only a single emitter without data association issues (no missed detections or false measurements). Each TDOA measurement defines a region of possible emitter locations around a unique hyperbola. This likelihood function is approximated by a Gaussian mixture, which leads to a dynamic bank of Kalman filters tracking algorithm. The FDOA measurements update relative probabilities and estimates of individual Kalman filters. This approach results in a better track state probability density function approximation by a Gaussian mixture, and tracking results near the Cramér–Rao lower bound. Proposed algorithm is also applicable in other cases of nonlinear information fusion. The performance of proposed Gaussian mixture approach is evaluated using a simulation study, and compared with a bank of EKF filters and the Cramér–Rao lower bound.**

***Index Terms*—Cramér–Rao bound, frequency difference of arrival (FDOA), geolocation, nonlinear estimation, sensor fusion, time difference of arrival (TDOA), tracking, Gaussian mixture presentation of measurements—integrated track splitting (GMM-ITS).**

I. Introduction

LOCALIZATION of an emitter on the surface of the Earth (geolocation) enables important applications, both military (surveillance) and civilian (localization, law enforcement, search and rescue, etc.). For a better visibility of emitters, it is often advantageous to mount sensors on unmanned aerial vehicles (UAVs). The UAVs may use small omnidirectional antennas and measure the time of arrival of signals at the receiver. A single measurement of this type is unable to provide any emitter-location information. When two sensors receive the same signal, the time difference of arrival (TDOA) can be calculated. Knowing the TDOA between the two sensors geolocalizes the emitter to a region around the points of a hyperbola. The TDOA measurements are especially suited to the geolocation of high-bandwidth emitters, e.g., radars. With the introduction of additional sensors (additional TDOA measurements), the emitter geolocation can be estimated at the intersection of two or more hyperbolae [1], [2]. Another approach is to use two moving sensors and nonlinear estimation [3] for geolocation using a sequence of TDOA measurements.

Emitter signal received by two sensors can also be utilized to simultaneously measure the frequency difference of arrival (FDOA), which is effectively the difference in received Doppler frequency offsets. A single FDOA measurement defines an area of possible emitter locations, whose shape and area depends on the sensor configuration (geometry and velocity vectors). The TDOA and FDOA measurements are often complementary in the sense that TDOA measurements are akin to the bearings measurements, and the FDOA measurements are (in certain sensor configurations) akin to the range measurements.

The FDOA and TDOA measurements may be jointly estimated from communication signals. Narrowband signals will have more precise FDOA measurements, and wideband signals will have more precise TDOA measurements, thus their combination will cover a wider range of emitters that may be tracked. The TDOA and FDOA measurements can be estimated using maximum-likelihood methods [4], [5], [7]. The Cramér–Rao bounds of the TDOA and FDOA measurement errors [4], [6], [8] are frequently so small that equipment-induced errors may be significant [9]. TDOA/FDOA observability criteria are discussed in [10]. In [11]–[13] different aspects of joint TDOA/FDOA estimation are investigated.

Estimating the location of an emitter from a combination of TDOA and FDOA measurements is a highly nonlinear problem. Often the approach is to use multiple simultaneous pairs of the TDOA/FDOA measurements (obtained by a number of sensors) in an overdetermined situation to estimate instantaneous location and velocity of the emitter [14]–[16]. This approach is not suitable when the emitter is mobile and a time sequence of the TDOA/FDOA measurement pairs is available. The position of an emitter can be estimated [17] using a sequence of bearing measurements from a single sensor which "outmaneuvers" the target. The sensor can also measure the Dopplerized radiated frequency [18]. The location method based on bearing measurements and the method based on frequency measurements differ substantially and present a different orientation of the error ellipsoids. Therefore, processing the combined set of bearing and frequency measurements leads to a significant integration gain in accuracy [19]. Based on the fusion of bearing and frequency measurements, this approach [18] gives an insight into the 3-D emitter localization problem. The combination of angle and frequency measurements improves the estimation accuracy significantly. A drawback of sufficiently accurate bearing measurements is the need of a large antenna aperture, which is not easy to mount on small UAVs. Instead of the bearings measurements, the TDOA measurements can be used. The TDOA/FDOA measurement pairs may be obtained by signals received by a single pair of UAVs. The receivers need only small omnidirectional apertures. In [20] and [9], the TDOA/FDOA measurements have

Manuscript received January 07, 2009; accepted October 16, 2009. First published November 20, 2009; current version published February 10, 2010. This work was supported by Fraunhofer FKIE under Contract 4500035757. The associate editor coordinating the review of this manuscript and approving it for publication was Dr. Zhi Tian.

D. Mušicki is with the Department of Electronic Information Systems Engineering, Hanyang University, Ansan, Kyunggido 426-791, Korea (e-mail: Darko.Musicki@gmail.com).

R. Kaune and W. Koch are with the Fraunhofer FKIE, Fraunhofer Institute for Communication, Information Processing and Ergonomics, Department SDF, Sensor Data and Information Fusion, 53343 Wachtberg, Germany (e-mail: regina.kaune@fkie.fraunhofer.de; wolfgang.koch@fkie.fraunhofer.de).

Digital Object Identifier 10.1109/TSP.2009.2037075

been used for geolocation using satellites, and the errors obtained by a single measurement pair are discussed.

In this paper a time sequence of the TDOA/FDOA measurement pairs is used to estimate the mobile emitter location and velocity. Proposed filter is also applicable when multiple pairs of UAVs simultaneously or asynchronously provide independent TDOA/FDOA measurement pairs, or when stationary sensors receive signals from a moving emitter.

The nonlinear estimation filter is based on the Gaussian mixture presentation of measurements—integrated track splitting (GMM-ITS) filter first published in [21]. GMM-ITS is a recursive procedure, derived using the Bayes formula. The nonlinear measurement likelihoods are approximated by Gaussian mixtures, and the emitter state probability density function (pdf) is approximated by a Gaussian mixture updated by a dynamic (track splitting) mixture of linear Kalman filters.

The GMM-ITS filter is used in [22] to integrate the TDOA and FDOA measurements to geolocate a stationary emitter. The likelihood of both TDOA and FDOA measurements are approximated by Gaussian mixtures. Although delivering excellent results for a stationary emitter, this method is not suitable for tracking a mobile emitter. This paper extends the GMM-ITS filter to fuse measurements when the likelihood of only one measurement (TDOA) may be represented by a Gaussian mixture and used to update the emitter state pdf in a standard GMM-ITS manner. The other measurement (FDOA) is used to alter the resulting emitter state pdf Gaussian mixture parameters.

The contributions of this paper are as follows.

- *Theoretical:* An extension of the GMM-ITS algorithm to also include (fuse) measurements whose likelihoods are not adequately approximated by a Gaussian mixture. The derivation of the extension is fully presented. This GMM-ITS filter extension may also be used for other nonlinear filtering applications where not all measurement types may be approximated by Gaussian mixtures.
- *Application:* Using the TDOA and the FDOA measurements for geolocation and tracking of mobile emitters which significantly improves upon industry standard and nears the theoretical Cramér–Rao-bounded performance limits. The filter can run in real time using relatively modest hardware.

This paper is organized as follows. The description of the scenario, the emitter trajectory model, and characterization of the TDOA and FDOA measurement models are presented in Section II. Section III presents the theoretical foundations for the fusion of the TDOA and FDOA measurements, as well as Gaussian mixture approximation of the TDOA measurement likelihood in the surveillance space. Section IV presents the details of the proposed estimator. Benchmarks (the EKF-based estimator and the Cramér–Rao lower bound) used for comparison with the proposed algorithm are presented in Section V. Simulation experiment in Section VI validates the approach. Finally, concluding remarks are given in Section VII.[1]

A. List of Acronyms

CRLB	Cramér–Rao lower bound
EKF	Extended Kalman filter
EKFb	A bank of extended Kalman filters
FDOA	Frequency difference of arrival
GMM	Gaussian mixture measurement presentation
ITS	Integrated track splitting
TDOA	Time difference of arrival

B. List of Global Symbols

c	Signal propagation speed
$\mathbf{e}_k$	Emitter kinematic state at k
$\hat{\mathbf{e}}_{k\,\vert\,k-1}, \mathbf{P}_{k\,\vert\,k-1}$	Prior state estimate, covariance at k
$\hat{\mathbf{e}}_{k\vert k}, \mathbf{P}_{k\vert k}$	Posterior state estimate, covariance at k
$\hat{\mathbf{e}}^t_{k\vert k}, \mathbf{P}^t_{k\vert k}$	emitter state estimate, covariance with only TDOA measurement applied at k
$\mathbf{F}$	State transition matrix
f_0	Signal carrier frequency
$\gamma_k, \mathbf{w}^t_k, \mathbf{R}^t_k$	Relative probability, mean and covariance of gth TDOA measurement component
$\mathbf{H}$	Position projection matrix; $\mathbf{x}_k = \mathbf{H}\mathbf{e}_k$
h^t, h^f	TDOA, FDOA measurement function
$\mathbf{H}^t, \mathbf{H}^f$	Jacobian of h^t, h^f
$\mathbf{i}^{(i)}$	Unit vector from sensor i to emitter
$\mathbf{I}$	Identity matrix
$\mathbf{J}$	Fisher information matrix
j	track component index
k	measurement sampling time index
$\mathcal{N}(\mathbf{x}; \mathbf{m}, \mathbf{P})$	Gaussian pdf of variable $\mathbf{x}$ with mean $\mathbf{m}$ and covariance $\mathbf{P}$
$\mathbf{Q}$	Plant noise covariance matrix
$\mathbf{r}^{(i)}$	Distance vector between emitter and sensor i
S^f_k, S^t_k	FDOA, TDOA EKF measurement innovation covariance at k
$\mathbf{S}^t_k$	TDOA ITS conceptual measurement innovation covariance at k
$\mathbf{s}^{(i)}$	Sensor i state
σ^2_t, σ^2_f	Covariance of u^t, u^f
$(\cdot)^\top$	Matrix $(\cdot)$ transpose
u^t, u^f	TDOA, FDOA measurement noise sample
$V_{\max}$	maximum speed constraint
$\mathbf{x}, \dot{\mathbf{x}}$	emitter position and velocity
$\mathbf{x}^{(i)}, \dot{\mathbf{x}}^{(i)}$	Sensor i position and velocity
$\xi_k(j)$	Posterior relative probability of track component j
$\xi^t_k(j)$	Relative probability of track component j after only TDOA measurement is applied
$\mathbf{y}^t_k$	Set of conceptual TDOA measurements in the surveillance space, defined by triplets $\{\gamma_k, \mathbf{w}^t_k, \mathbf{R}^t_k\}$
$\mathbf{Z}^k$	Set of measurements taken up to and including time k

[1]Some portions of this paper also appear in [22]

$\mathbf{z}_k$	Set of measurements taken at k
z_k^t, z_k^f	TDOA, FDOA measurement at time k

II. Problem Statement

A moving emitter exists on the surface of the Earth. In this paper we assume a flat Earth with the sensors located in the Earth plane. These assumptions considerably simplify the geometry, without influencing the conclusions. The Earth curvature, geographical relief, and the height of the sensors can be accommodated in a straightforward manner. The kinematic state of the emitter at time k is

$$\mathbf{e}_k^\top = [\,\mathbf{x}_k^\top \quad \dot{\mathbf{x}}_k^\top\,] \tag{1}$$

where $\mathbf{x}_k$ denotes the emitter position, $\dot{\mathbf{x}}_k$ the emitter velocity, and $^\top$ denotes the matrix transpose. Define the "position projection" matrix $\mathbf{H}$ by $\mathbf{x}_k = \mathbf{H}\mathbf{e}_k$. The emitter trajectory at time k is

$$\mathbf{e}_k = \mathbf{F}_{k-1}\mathbf{e}_{k-1} + \boldsymbol{\nu}_{k-1} \tag{2}$$

where the plant noise sequence $\boldsymbol{\nu}_k$ is assumed to be a zero-mean and white Gaussian sequence with covariance $\mathbf{Q}_k$, not correlated with any measurement noise sequence. The emitter is observed by two moving sensors with the state vectors at time k

$$\mathbf{s}_k^{(i)\top} = \left[\,\mathbf{x}_k^{(i)\top} \quad \dot{\mathbf{x}}_k^{(i)\top}\,\right], \qquad i = 1, 2 \tag{3}$$

where $\mathbf{x}_k^{(i)}$ and $\dot{\mathbf{x}}_k^{(i)}$ denote sensor i known position and speed vectors respectively.

A. Time Difference of Arrival

The distance vector between the emitter and sensor i at time k is $\mathbf{r}_k^{(i)} = \mathbf{x}_k - \mathbf{x}_k^{(i)}$, and the time delay of signal received at sensor i is $\|\mathbf{r}_k^{(i)}\|/c$, with c denoting the signal propagation speed. The TDOA is the difference between corresponding time intervals and is given by

$$h^t\left(\mathbf{e}_k; \mathbf{s}_k^{(1)}, \mathbf{s}_k^{(2)}\right) = \left(\|\mathbf{r}_k^{(1)}\| - \|\mathbf{r}_k^{(2)}\|\right)/c. \tag{4}$$

In Fig. 1 all points on the solid line have the same distance difference to the two sensors and, therefore, the same true time difference of arrival. The TDOA measurement at time k is

$$z_k^t = h^t\left(\mathbf{e}_k; \mathbf{s}_k^{(1)}, \mathbf{s}_k^{(2)}\right) + u_k^t \tag{5}$$

with additive zero-mean white Gaussian noise samples u_k^t with covariance σ_t^2 and uncorrelated to the FDOA measurement noise.

B. Frequency Difference of Arrival

The Doppler shift of the signal received by sensor i at time k is proportional to the radial component of the emitter relative velocity. Let

$$\mathbf{i}_k^{(i)} = \frac{\mathbf{r}_k^{(i)}}{\|\mathbf{r}_k^{(i)}\|}, \qquad i = 1, 2 \tag{6}$$

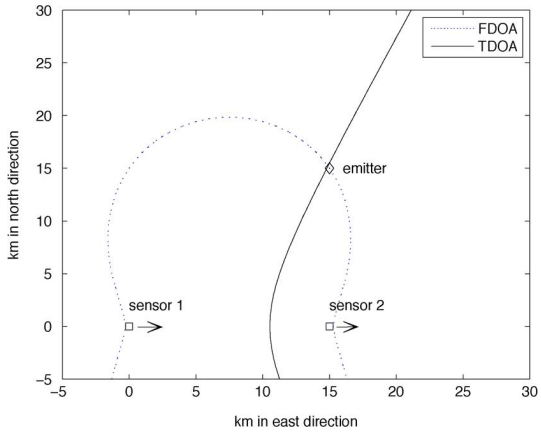

Fig. 1. Constant FDOA and TDOA emitter location curves.

denote the unit vector from sensor i at time k to the emitter. The Doppler shift observed by sensor i is

$$\frac{f_0}{c}\left(\mathbf{i}_k^{(i)}\right)^\top (\dot{\mathbf{x}}_k^{(i)} - \dot{\mathbf{x}}_k) \tag{7}$$

where f_0 denotes the signal carrier frequency. Subtracting the Doppler frequency shifts from different sensors, the FDOA equals

$$\Delta f_k^{(1),(2)} = \frac{f_0}{c} \times \left((\mathbf{i}_k^{(1)})^\top \left(\dot{\mathbf{x}}_k^{(1)} - \dot{\mathbf{x}}_k\right) - (\mathbf{i}_k^{(2)})^\top (\dot{\mathbf{x}}_k^{(2)} - \dot{\mathbf{x}}_k)\right). \tag{8}$$

The FDOA is a nonlinear function of emitter state

$$\Delta f_k^{(1),(2)} = h^f\left(\mathbf{e}_k; \mathbf{s}_k^{(1)}, \mathbf{s}_k^{(2)}\right). \tag{9}$$

An example of a constant FDOA curve is shown by the dotted curve on Fig. 1; the arrows show the velocity direction of the sensors. In this example, the emitter is stationary, the TDOA signal takes the (approximate) role of the bearing, and the FDOA signal takes the (approximate) role of the distance measurement.

The FDOA measurements may be modeled by adding zero-mean white Gaussian noise to the true FDOA values

$$z_k^f = h^f(\mathbf{e}_k; \mathbf{s}_k^{(1)}, \mathbf{s}_k^{(2)}) + u_k^f \tag{10}$$

with u_k^f zero-mean white Gaussian process with covariance σ_f^2.

C. TDOA and FDOA Measurement Errors

Given relatively mild conditions [5]–[8], which include sufficiently large time/bandwidth products of the received signal and noise processes, and high enough integrated signal-to-noise ratio, the CRLB of joint TDOA/FDOA estimation is diagonal, and the TDOA and FDOA estimates are asymptotically uncorrelated.

Certain TDOA/FDOA estimators [4], [5], [7] approach the CRLB, with the consequent approximate noncorrelation between the TDOA and FDOA measurement errors. As in [14]–[16] we assume that TDOA and FDOA measurements are obtained by such estimators, and that TDOA and FDOA

errors are additive, Gaussian with zero-mean and mutually independent (uncorrelated).

The CRLB of TDOA and FDOA measurement errors are [4]

$$\begin{aligned}\sigma_t^{-1} &= \beta\sqrt{BTS_i}\\ \sigma_f^{-1} &= T_e\sqrt{BTS_i}\end{aligned} \tag{11}$$

respectively, where B denotes the emitter signal bandwidth, T denotes the TDOA/FDOA estimator integration period, and S_i denotes the input signal-to-noise ratio. The rms bandwidth and duration of the emitter signal are

$$\begin{aligned}\beta &= 2\pi\sqrt{\frac{\int_{-\infty}^{\infty} f^2 W_s(f)\mathrm{d}f}{\int_{-\infty}^{\infty} W_s(f)\mathrm{d}f}}\\ T_e &= 2\pi\sqrt{\frac{\int_{-\infty}^{\infty} t^2|a(t)|^2\mathrm{d}t}{\int_{-\infty}^{\infty}|a(t)|^2\mathrm{d}t}}\end{aligned} \tag{12}$$

where $W_s(f)$ and $|a(t)|$ denote the emitter signal power spectrum and the complex envelope respectively.

Given the emitter signal bandwidth $B = 25$ kHz, and assuming the integration time $T = 2$ s, the efficient TDOA/FDOA estimator calculation [4] requires half a million of complex multiplications and additions per second, well within current technology capabilities. The data transmission requirements for two streams of 30 000 complex samples per second are also available. Given the input signal-to-noise ratio of $S_i = 0$ dB, the rms error bounds are $\sigma_t = 98$ ns (differential range rms error of $\approx$30 m) and $\sigma_f = 1.2$ mHz (given the carrier frequency of $f_0 = 100$ MHz this translates to differential radial velocity $\approx$3.7 mm/s). Practically achievable measurement errors also depend on the stability of other components in the signal processing chain, which is beyond the scope of this paper [9], [10].

III. Measurement Fusion

At each measurement time k, the TDOA z_k^t and the FDOA z_k^f measurements of emitter position $\mathbf{e}_k$ are simultaneously taken. Denote by $\mathbf{z}_k$ the measurement pair taken at time $k, \mathbf{z}_k = \{z_k^t, z_k^f\}$. Denote by $\mathbf{Z}^k$ the set of measurement pairs taken up to and including time k; $\mathbf{Z}^k = \mathbf{z}_k \cup \mathbf{Z}^{k-1}$ with $\mathbf{Z}^0 = \{\}$.

In this section we first explore information fusion issues when using measurement pair $\mathbf{z}_k$, i.e., the measurement likelihood (Section III-A) and the Bayes state update (Section III-B). We show the equivalence between applying both measurements simultaneously and first applying the TDOA measurement z_k^t, followed by the FDOA measurement z_k^f. The Gaussian mixture approximation of the TDOA measurement likelihood in the surveillance space is then presented.

A. Measurement Likelihoods

Under the white measurement noise assumption, conditional measurement likelihood depends only on current state, and does not depend on previous measurements

$$p(\mathbf{z}_k|\mathbf{e}_k, \mathbf{Z}^{k-1}) = p(\mathbf{z}_k|\mathbf{e}_k) \tag{13}$$

where $p(\cdot)$ denotes the pdf. The TDOA and the FDOA measurements are mutually independent, given the emitter state

$$\begin{aligned}p(\mathbf{z}_k|\mathbf{e}_k) &= p(z_k^t, z_k^f|\mathbf{e}_k)\\ &= p(z_k^t|\mathbf{e}_k)p(z_k^f|\mathbf{e}_k).\end{aligned} \tag{14}$$

Unconditional likelihoods of the TDOA and the FDOA measurements are not mutually independent

$$\begin{aligned}p(\mathbf{z}_k|\mathbf{Z}^{k-1}) &= p(z_k^t, z_k^f|\mathbf{Z}^{k-1})\\ &= p(z_k^t|\mathbf{Z}^{k-1})p(z_k^f|z_k^t, \mathbf{Z}^{k-1})\end{aligned} \tag{15}$$

and are obtained by

$$p(z_k^t|\mathbf{Z}^{k-1}) = \int_{\mathbf{e}_k} p(z_k^t|\mathbf{e}_k)p(\mathbf{e}_k|\mathbf{Z}^{k-1})\mathrm{d}\mathbf{e}_k \tag{16}$$

$$p(z_k^f|z_k^t, \mathbf{Z}^{k-1}) = \int_{\mathbf{e}_k} p(z_k^f|\mathbf{e}_k)p(\mathbf{e}_k|z_k^t, \mathbf{Z}^{k-1})\mathrm{d}\mathbf{e}_k \tag{17}$$

where $p(\mathbf{e}_k|\mathbf{Z}^{k-1})$ is the propagated state pdf from time $k-1$ to time k, and $p(\mathbf{e}_k|z_k^t, \mathbf{Z}^{k-1})$ is the state pdf when only TDOA measurement z_k^t has been applied to $p(\mathbf{e}_k|\mathbf{Z}^{k-1})$.

B. Bayes Update

A posteriori state estimate pdf at time k is denoted by

$$\begin{aligned}p(\mathbf{e}_k|\mathbf{Z}^k) &= p(\mathbf{e}_k|\mathbf{z}_k, \mathbf{Z}^{k-1})\\ &= p(\mathbf{e}_k|z_k^t, z_k^f, \mathbf{Z}^{k-1})\end{aligned} \tag{18}$$

and is calculated by using the well-known Bayes formula

$$p(\mathbf{e}_k|\mathbf{Z}^k) = \frac{p(z_k^t, z_k^f|\mathbf{e}_k)}{p(z_k^t, z_k^f|\mathbf{Z}^{k-1})}p(\mathbf{e}_k|\mathbf{Z}^{k-1}). \tag{19}$$

Representing conditional and unconditional joint measurement likelihoods by (14) and (15) respectively, $p(\mathbf{e}_k|\mathbf{Z}^k)$ is expressed by

$$\frac{p\left(z_k^t|\mathbf{e}_k\right)p\left(z_k^f|\mathbf{e}_k\right)}{p\left(z_k^t|\mathbf{Z}^{k-1}\right)p\left(z_k^f|z_k^t, \mathbf{Z}^{k-1}\right)}p(\mathbf{e}_k|\mathbf{Z}^{k-1}). \tag{20}$$

Applying the TDOA measurement first results in

$$p\left(\mathbf{e}_k|z_k^t, \mathbf{Z}^{k-1}\right) = \frac{p\left(z_k^t|\mathbf{e}_k\right)}{p\left(z_k^t|\mathbf{Z}^{k-1}\right)}p\left(\mathbf{e}_k|\mathbf{Z}^{k-1}\right) \tag{21}$$

and rearranging (20) we obtain

$$p(\mathbf{e}_k|\mathbf{Z}^k) = \frac{p\left(z_k^f|\mathbf{e}_k\right)}{p\left(z_k^f|z_k^t, \mathbf{Z}^{k-1}\right)}p\left(\mathbf{e}_k|z_k^t, \mathbf{Z}^{k-1}\right). \tag{22}$$

In other words, an *a posteriori* state estimate pdf when information of both TDOA z_k^t and FDOA z_k^f measurements are applied can also be obtained if we first apply the TDOA measurement z_k^t only, followed by applying the FDOA measurement z_k^f to the result.

C. TDOA Measurement GMM Representation

The TDOA measurement z_k^t is nonlinear, as its conditional likelihood $p(z_k^t|\mathbf{e}_k)$ is not a Gaussian function of state $\mathbf{e}_k$. We choose here to use the GMM-ITS [21], [22] filter to apply the TDOA measurement. The GMM-ITS has two parts; the first one is approximating the measurement likelihood by a Gaussian mixture (GMM) in the surveillance space, and the second one is using the GMM likelihood approximation to update the track splitting filter (ITS). This subsection deals with the first part, the Gaussian measurement mixture (GMM) approximation; the second part is detailed in Section IV-C.

Measurement z_k^t is known, as it is returned by the sensor. The conditional measurement likelihood $p(z_k^t|\mathbf{e}_k)$ is a function of emitter position $\mathbf{He}_k$ only, as per (5)

$$p(z_k^t|\mathbf{e}_k) = f_{zt}(\mathbf{He}_k). \tag{23}$$

Function $f_{zt}(\mathbf{He}_k)$ is nonnegative and does not necessarily integrate to one

$$\begin{aligned} f_{zt}(\mathbf{He}_k) &\geqq 0 \\ \int_{\mathbf{e}_k} f_{zt}(\mathbf{He}_k)\mathrm{d}(\mathbf{He}_k) &\lesseqgtr 1. \end{aligned} \tag{24}$$

Therefore $f_{zt}(\mathbf{He}_k)$ is just a density, not a probability density function of the emitter position $\mathbf{He}_k$. Equation (21) becomes

$$p(\mathbf{e}_k|z_k^t, \mathbf{Z}^{k-1}) = \frac{f_{zt}(\mathbf{He}_k)p(\mathbf{e}_k|\mathbf{Z}^{k-1})}{\int_{\mathbf{e}_k} f_{zt}(\mathbf{He}_k)p(\mathbf{e}_k|\mathbf{Z}^{k-1})\mathrm{d}\mathbf{e}_k} \tag{25}$$

from which it is apparent that multiplying $f_{zt}(\mathbf{He}_k)$ by any constant >0 will not change $p(\mathbf{e}_k|z_k^t, \mathbf{Z}^{k-1})$. GMM representation seeks to approximate $f_{zt}(\mathbf{He}_k)$ by a Gaussian mixture $f_{yt}(\mathbf{He}_k)$ [23]

$$f_{zt}(\mathbf{He}_k) \approx C f_{yt}(\mathbf{He}_k) \tag{26}$$

where C is a constant independent of $\mathbf{e}_k$, and

$$p(\mathbf{y}_k^t|\mathbf{e}_k) \triangleq f_{yt}(\mathbf{He}_k) = \sum_{g=1}^{G_k} \gamma_k(g) p(\mathbf{w}_k^t(g)|\mathbf{e}_k) \tag{27}$$

where G_k denotes the number of measurement components and

$$p(\mathbf{w}_k^t(g)|\mathbf{e}_k) = \mathcal{N}\left(\mathbf{w}_k^t(g); \mathbf{He}_k, \mathbf{R}_k^t(g)\right) \tag{28}$$

where $\mathcal{N}(\mathbf{x}; \mathbf{m}, \mathbf{P})$ denotes the Gaussian pdf of variable $\mathbf{x}$ with mean $\mathbf{m}$ and covariance $\mathbf{P}$. Measurement z_k^t and its covariance σ_t^2 are replaced by a set $\mathbf{y}_k^t$ of G_k triplets $\{\gamma_k(g), \mathbf{w}_k^t(g), \mathbf{R}_k^t(g)\}$. Each triplet corresponds to a conceptual "measurement" in the surveillance space $\mathbf{He}_k$ and is termed here a measurement component. Measurement component g has "value" $\mathbf{w}_k^t(g)$ and "error" covariance matrix $\mathbf{R}_k^t(g)$. The measurement components are mutually exclusive and component g is correct with probability $\gamma_k(g)$. Therefore

$$\sum_{g=1}^{G_k} \gamma_k(g) = 1; \qquad \gamma_k(g) \geq 0 \tag{29}$$

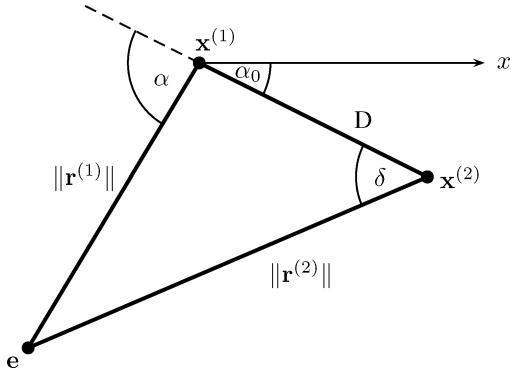

Fig. 2. TDOA geometry.

although, strictly from the Bayes equation point, this constraint is not necessary. A procedure which maps TDOA measurement z_k^t with covariance σ_t^2 into GMM presentation defined by (27) consists of three steps.

- "Draw" curves defined by $\|\mathbf{r}_k^{(1)}\| - \|\mathbf{r}_k^{(2)}\| = c(z_k^t \pm \sigma_t)$ in the surveillance space $\mathbf{He}_k$.
- Divide the curves into segments.
- Inscribe an ellipsoid in the space between each pair of corresponding segments. Each ellipsoid is the footprint of a measurement component.

These steps are described in the remainder of this section. Although this approach is pragmatic and may be improved by future research, it results in a computationally efficient algorithm.

There are several ways to construct the TDOA curve defined by $\|\mathbf{r}^{(1)}\| - \|\mathbf{r}^{(2)}\| = \Delta r$, where Δr is constant, and is depicted by the solid curve in Fig. 1. In this paper we use the parametric constant TDOA curve construction. Consider the situation in Fig. 2.

Assuming known angle α (the parameter)

$$\begin{aligned} \|\mathbf{r}^{(2)}\| - \|\mathbf{r}^{(1)}\| &= \Delta r \\ \|\mathbf{r}^{(2)}\| \sin(\delta) &= \|\mathbf{r}^{(1)}\| \sin(\alpha) \\ \|\mathbf{r}^{(2)}\| \cos(\delta) - \|\mathbf{r}^{(1)}\| \cos(\alpha) &= D \end{aligned} \tag{30}$$

holds and may be solved as

$$\|\mathbf{r}^{(1)}(\alpha, \Delta r)\| = \frac{D^2 - (\Delta r)^2}{2(\Delta r - D\cos(\alpha))} \tag{31}$$

where D denotes the baseline distance between the two sensors. Given parameter α, we can calculate $\|\mathbf{r}^{(1)}\|$ and then the emitter location as

$$\mathbf{He}(\alpha, \Delta r) = \mathbf{x}^{(1)} - \|\mathbf{r}^{(1)}(\alpha, \Delta r)\| \begin{bmatrix} \cos(\alpha - \alpha_0) \\ \sin(\alpha - \alpha_0) \end{bmatrix} \tag{32}$$

where α_0 denotes the slant angle of sensors baseline. By letting α assume values from its range, defined by the boundaries of surveillance region, the constant TDOA curve may be constructed.

A result of drawing two curves defined by $\Delta r = c(z_k^t \pm \sigma_t)$ in surveillance space is shown by dotted lines on Fig. 3. As we are segmenting each curve, we only need values of potential emitter

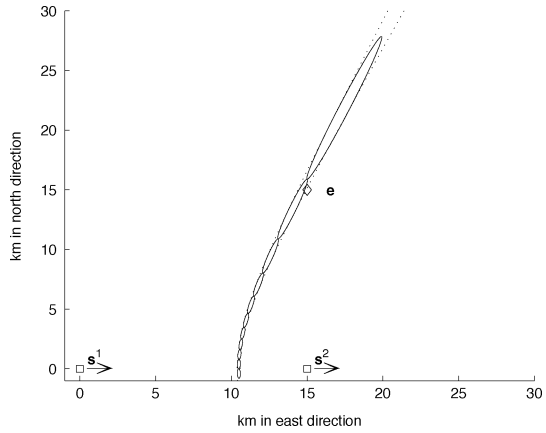

Fig. 3. TDOA $\pm\sigma$ uncertainty in surveillance space.

locations $\mathbf{He}(\alpha, \Delta r)$, (32) at a limited set of angles denoted here by $\boldsymbol{\alpha} = [\alpha_1 \cdots \alpha_{G+1}]^\top$.

An ellipsoid is inscribed within each quadrangle formed by one pair of points on each curve shown in Fig. 3 corresponding to the same angles. Denote the end points of one corresponding pair of segments by $\mathbf{x}_1, \ldots, \mathbf{x}_4$. As per (32), they are equal to

$$\begin{bmatrix} \mathbf{x}_1(g) \\ \mathbf{x}_2(g) \\ \mathbf{x}_3(g) \\ \mathbf{x}_4(g) \end{bmatrix} = \begin{bmatrix} \mathbf{He}(\alpha_g, cz_k^t + c\sigma_t) \\ \mathbf{He}(\alpha_{g+1}, cz_k^t + c\sigma_t) \\ \mathbf{He}(\alpha_g, cz_k^t - c\sigma_t) \\ \mathbf{He}(\alpha_{g+1}, cz_k^t - c\sigma_t) \end{bmatrix}. \tag{33}$$

We want to define the measurement component g whose footprint is the ellipsoid inscribed within points $\mathbf{x}_1, \ldots, \mathbf{x}_4$.

The end points of one semiaxis of the inscribed ellipsoid are defined by

$$\begin{aligned} \mathbf{x}_{c1} &= (\mathbf{x}_1 + \mathbf{x}_3)/2 \\ \mathbf{x}_{c2} &= (\mathbf{x}_2 + \mathbf{x}_4)/2. \end{aligned} \tag{34}$$

Length D_c and unit vector $\mathbf{i}(\alpha_c)$ of this semiaxis of the ellipsoid are

$$\begin{aligned} \Delta\mathbf{x}_c &= \mathbf{x}_{c1} - \mathbf{x}_{c2} \\ D_c &= ||\Delta\mathbf{x}_c||/2 \\ \mathbf{i}(\alpha_c) &\triangleq \begin{bmatrix} \cos(\alpha_c) \\ \sin(\alpha_c) \end{bmatrix} = \frac{\Delta\mathbf{x}_c}{||\Delta\mathbf{x}_c||}. \end{aligned} \tag{35}$$

The length D_s of the other semiaxis is given by

$$\begin{aligned} &\begin{bmatrix} -\sin(\alpha_c) \\ \cos(\alpha_c) \end{bmatrix}^\top \frac{1}{2}\left(\frac{\mathbf{x}_1 - \mathbf{x}_3}{2} + \frac{\mathbf{x}_2 - \mathbf{x}_4}{2}\right) \\ &\qquad = \mathbf{i}(\alpha_c + \pi/2)^\top \left(\frac{\mathbf{x}_1 + \mathbf{x}_2 - \mathbf{x}_3 - \mathbf{x}_4}{4}\right). \end{aligned} \tag{36}$$

The center of the inscribed ellipsoid is given by

$$\mathbf{w}_k^t(g) = 0.5(\mathbf{x}_{c1} + \mathbf{x}_{c2}) \tag{37}$$

which is also the mean of the measurement component g corresponding to the ellipsoid. Denote α rotation matrix by $\mathbf{T}(\alpha) = [\mathbf{i}(\alpha) \quad \mathbf{i}(\alpha + \pi/2)]$. The covariance matrix of measurement component g is

$$\mathbf{R}_k^t(g) = \mathbf{T}(\alpha_c)\begin{bmatrix} D_c^2 & 0 \\ 0 & D_s^2 \end{bmatrix}\mathbf{T}(\alpha_c)^\top. \tag{38}$$

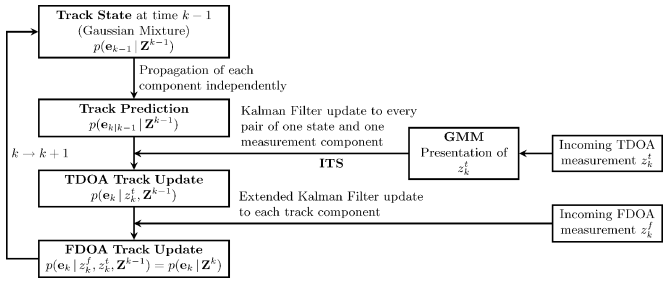

Fig. 4. One cycle of GMM-ITS-based TDOA/FDOA filter.

Without any prior information, the emitter position is equally probable at any point of the observation space. The probability that the emitter is within the footprint of a measurement component is proportional to the area of the footprint

$$\gamma(g) \propto \sqrt{|\mathbf{R}_k^t(g)|} \tag{39}$$

where $|\cdot|$ denotes the determinant.

IV. Track Propagation and Measurement Update

The non-Gaussian emitter state pdf is approximated by a Gaussian mixture [23] of track components. We assume linear emitter trajectory propagation, defined by (2). The TDOA measurement likelihood is represented by a Gaussian mixture of TDOA measurement components in the surveillance space. Each TDOA measurement component is applied to each track component by a standard Kalman filter, which creates new track components. Application of Kalman filters reduces prior track component covariance matrices. The nonlinear FDOA measurement is then applied to each new track component by an extended Kalman filter (EKF). The EKF in this case linearizes the measurement equation around the TDOA-updated component mean state projection, and the EKF linearization domain is reduced due to the TDOA measurement application. It is thus advantageous to apply the TDOA measurement before the FDOA measurement.

Fig. 4 shows one cycle of the GMM-ITS-based TDOA/FDOA filter.

A. Track State

A posteriori track state pdf at time $k-1$ (after processing the measurement set $\mathbf{Z}^{k-1}$) is approximated by a Gaussian mixture, defined by

$$\begin{aligned} p(\mathbf{e}_{k-1}|\mathbf{Z}^{k-1}) &= \sum_{j=1}^{J_{k-1}} \xi_{k-1}(j) p(\mathbf{e}_{k-1}|j, \mathbf{Z}^{k-1}) \\ p(\mathbf{e}_{k-1}|j, \mathbf{Z}^{k-1}) &= \mathcal{N}(\mathbf{e}_{k-1}; \hat{\mathbf{e}}_{k-1|k-1}(j), \mathbf{P}_{k-1|k-1}(j)) \end{aligned} \tag{40}$$

where each Gaussian pdf is termed a track component, j indexes and identifies (depending on the context) track components, J_{k-1} denotes the number of track components, and $\hat{\mathbf{e}}_{k-1|k-1}(j)$ and $\mathbf{P}_{k-1|k-1}(j)$ are the mean and the covariance of track component j. Relative component probabilities $\xi_{k-1}(j)$ are constrained by

$$\sum_{j=1}^{J_{k-1}} \xi_{k-1}(j) = 1; \xi_{k-1}(j) \geq 0. \tag{41}$$

Thus $p(\mathbf{e}_{k-1}|\mathbf{Z}^{k-1})$ is positive and integrates to one.

B. Track Prediction

The Chapman-Kolmogoroff equation is applied to propagate emitter state pdf from $k-1$ to k

$$p(\mathbf{e}_k|\mathbf{Z}^{k-1}) = \int_{\mathbf{e}_{k-1}} p(\mathbf{e}_k|\mathbf{e}_{k-1}) p(\mathbf{e}_{k-1}|\mathbf{Z}^{k-1}) \mathrm{d}\mathbf{e}_{k-1}. \quad (42)$$

Substituting (40) into (42) and exchanging integration and summation yield

$$\begin{aligned} p(\mathbf{e}_k|\mathbf{Z}^{k-1}) &= \sum_{j=1}^{J_{k-1}} \xi_{k-1}(j) \\ &\quad \times \int_{\mathbf{e}_{k-1}} p(\mathbf{e}_k|\mathbf{e}_{k-1}) p(\mathbf{e}_{k-1}|j, \mathbf{Z}^{k-1}) \mathrm{d}\mathbf{e}_{k-1} \\ &= \sum_{j=1}^{J_{k-1}} \xi_{k-1}(j) p(\mathbf{e}_k|j, \mathbf{Z}^{k-1}). \end{aligned} \quad (43)$$

From (2)

$$p(\mathbf{e}_k|\mathbf{e}_{k-1}) = \mathcal{N}(\mathbf{e}_k; \mathbf{F}_{k-1}\mathbf{e}_{k-1}, \mathbf{Q}_{k-1}) \quad (44)$$

we obtain

$$p(\mathbf{e}_k|j, \mathbf{Z}^{k-1}) = \mathcal{N}\left(\mathbf{e}_k; \hat{\mathbf{e}}_{k\,|\,k-1}(j), \mathbf{P}_{k\,|\,k-1}(j)\right) \quad (45)$$

where each component j propagates independently and in a linear manner

$$\begin{aligned} \hat{\mathbf{e}}_{k\,|\,k-1}(j) &= \mathbf{F}_{k-1}\hat{\mathbf{e}}_{k-1|k-1}(j) \\ \mathbf{P}_{k\,|\,k-1}(j) &= \mathbf{F}_{k-1}\mathbf{P}_{k-1|k-1}(j)\mathbf{F}_{k-1}^{\top} + \mathbf{Q}_{k-1}. \end{aligned} \quad (46)$$

C. TDOA Track Update

This corresponds to applying measurement z_k^t on the propagated pdf $p(\mathbf{e}_k|\mathbf{Z}^{k-1})$ to obtain $p(\mathbf{e}_k|z_k^t, \mathbf{Z}^{k-1})$. Measurement z_k^t likelihood is approximated (up to the proportionality constant) by a Gaussian mixture in the surveillance space (27). The propagated state estimate pdf $p(\mathbf{e}_k|\mathbf{Z}^{k-1})$ is approximated by a Gaussian mixture in state space (43). Nonlinear state update is approximated by applying linear estimator (Kalman filter update) to every pair of one propagated track component and one measurement component. Each pair creates a new track component for subsequent updates and propagations.

Applying Bayes equation (21) and (26), we have

$$\begin{aligned} p(\mathbf{e}_k|z_k^t, \mathbf{Z}^{k-1}) &= \frac{p(z_k^t|\mathbf{e}_k)}{p(z_k^t|\mathbf{Z}^{k-1})} p(\mathbf{e}_k|\mathbf{Z}^{k-1}) \\ &= \frac{p(\mathbf{y}_k^t|\mathbf{e}_k)}{p(\mathbf{y}_k^t|\mathbf{Z}^{k-1})} p(\mathbf{e}_k|\mathbf{Z}^{k-1}). \end{aligned} \quad (47)$$

Applying (27) and (43), we have

$$\begin{aligned} p(\mathbf{e}_k|z_k^t, \mathbf{Z}^{k-1}) &= \sum_{j=1}^{J_{k-1}} \sum_{g=1}^{G_k} \xi_{k-1}(j)\gamma_k(g) \\ &\quad \times \frac{p(\mathbf{w}_k^t(g)|\mathbf{e}_k) p(\mathbf{e}_k|j, \mathbf{Z}^{k-1})}{p(\mathbf{y}_k^t|\mathbf{Z}^{k-1})}. \end{aligned} \quad (48)$$

Unconditional TDOA measurement likelihood is

$$p\left(\mathbf{y}_k^t|\mathbf{Z}^{k-1}\right) = \int_{\mathbf{e}_k} p\left(\mathbf{y}_k^t|\mathbf{e}_k\right) p(\mathbf{e}_k|\mathbf{Z}^{k-1}) \mathrm{d}\mathbf{e}_k \quad (49)$$

$$\begin{aligned} p(\mathbf{y}_k^t|\mathbf{Z}^{k-1}) &= \sum_{g=1}^{G_k} \gamma_k(g) \sum_{j=1}^{J_{k-1}} \xi_{k-1}(j) \\ &\quad \times \int_{\mathbf{e}_k} p(\mathbf{w}_k^t(g)|\mathbf{e}_k) p(\mathbf{e}_k|j, \mathbf{Z}^{k-1}) \mathrm{d}\mathbf{e}_k \end{aligned} \quad (50)$$

which is formally equal to

$$p(\mathbf{y}_k^t|\mathbf{Z}^{k-1}) = \sum_{g=1}^{G_k} \sum_{j=1}^{J_{k-1}} \gamma_k(g)\xi_{k-1}(j) p(\mathbf{w}_k^t(g)|j, \mathbf{Z}^{k-1}) \quad (51)$$

with

$$p(\mathbf{w}_k^t(g)|j, \mathbf{Z}^{k-1}) = \mathcal{N}\left(\mathbf{w}_k^t(g); \mathbf{H}\hat{\mathbf{e}}_{k\,|\,k-1}(j), \mathbf{S}_k^t(j,g)\right) \quad (52)$$

and covariance matrix of measurement g innovation with respect to track component j is

$$\mathbf{S}_k^t(j,g) = \mathbf{H}\mathbf{P}_{k\,|\,k-1}(j)\mathbf{H}^{\top} + \mathbf{R}_k^t(g). \quad (53)$$

Multiplying and dividing (48) by $p(\mathbf{w}_k^t(g)|j, \mathbf{Z}^{k-1})$ and applying Bayes formula again, we get

$$\begin{aligned} p\left(\mathbf{e}_k|z_k^t, \mathbf{Z}^{k-1}\right) &= \sum_{j=1}^{J_{k-1}} \sum_{g=1}^{G_k} \frac{\xi_{k-1}(j)\gamma_k(g) p\left(\mathbf{w}_k^t(g)|j, \mathbf{Z}^{k-1}\right)}{p\left(\mathbf{y}_k^t|\mathbf{Z}^{k-1}\right)} \\ &\quad \times p\left(\mathbf{e}_k|j, \mathbf{w}_k^t(g), \mathbf{Z}^{k-1}\right) \end{aligned} \quad (54)$$

which is reshaped to

$$p\left(\mathbf{e}_k|z_k^t, \mathbf{Z}^{k-1}\right) = \sum_{j^+=1}^{J_k} \xi_k^t(j^+) p\left(\mathbf{e}_k|j^+, z_k^t, \mathbf{Z}^{k-1}\right) \quad (55)$$

where $j^+ \equiv \{g, j\}$ is the index into new track components created by applying the TDOA GMM measurement component g to the propagated track component j. Each TDOA measurement component g uses the Kalman filter update of each existing track component j to create one new track component j^+. The number of new track components of *a posteriori* track pdf at time k is $J_k = J_{k-1} \cdot G_k$ and

$$\xi_k^t(j^+) = \frac{\xi_{k-1}(j)\gamma_k(g) p\left(\mathbf{w}_k^t(g)|j, \mathbf{Z}^{k-1}\right)}{p\left(\mathbf{y}_k^t|\mathbf{Z}^{k-1}\right)} \quad (56)$$

$$p(\mathbf{e}_k|j^+, z_k^t, \mathbf{Z}^{k-1}) = \mathcal{N}\left(\mathbf{e}_k; \hat{\mathbf{e}}_{k|k}^t(j^+), \mathbf{P}_{k|k}^t(j^+)\right) \quad (57)$$

where $\hat{\mathbf{e}}_{k|k}^t(j^+)$ and $\mathbf{P}_{k|k}^t(j^+)$ are the mean value and the covariance matrix of new track component j^+ respectively, calculated by the Kalman filter update

$$\begin{aligned} \hat{\mathbf{e}}_{k|k}^t(j^+) &= \hat{\mathbf{e}}_{k\,|\,k-1}(j) + \mathbf{K}_k^t(j^+)\left(\mathbf{w}_k^t(g) - \mathbf{H}\hat{\mathbf{e}}_{k\,|\,k-1}(j)\right) \\ \mathbf{P}_{k|k}^t(j^+) &= \left(\mathbf{I} - \mathbf{K}_k^t(j^+)\mathbf{H}\right)\mathbf{P}_{k\,|\,k-1}(j) \end{aligned} \quad (58)$$

where $\mathbf{S}_k^t(j,g)$ is defined by (53) and the Kalman gain is

$$\mathbf{K}_k^t(j^+) = \mathbf{P}_{k\,|\,k-1}(j)\mathbf{H}^{\top}\mathbf{S}_k^t(j,g)^{-1}. \quad (59)$$

Relative probabilities $\xi_k^t(j^+) \equiv \xi_k^t(\{g,j\})$ satisfy

$$\sum_{j^+=1}^{J_k} \xi_k^t(j^+) = 1. \quad (60)$$

D. FDOA Track Update

The FDOA measurement z_k^f is applied to $p(\mathbf{e}_k|z_k^t, \mathbf{Z}^{k-1})$ to obtain $p(\mathbf{e}_k|\mathbf{z}_k)$. For this operation, *a priori* state estimate pdf is $p(\mathbf{e}_k|z_k^t, \mathbf{Z}^{k-1})$, which is a Gaussian mixture defined by (55)–(59). Using the Bayes equation and the Gaussian mixture track state (55) we have

$$\begin{aligned} p(\mathbf{e}_k|z_k^f, z_k^t, \mathbf{Z}^{k-1}) &= \frac{p(z_k^f|\mathbf{e}_k)}{p(z_k^f|z_k^t, \mathbf{Z}^{k-1})} p(\mathbf{e}_k|z_k^t, \mathbf{Z}^{k-1}) \\ &= \frac{p(z_k^f|\mathbf{e}_k)}{p(z_k^f|z_k^t, \mathbf{Z}^{k-1})} \\ &\quad \times \sum_{j^+=1}^{J_k} \xi_k^t(j^+) p(\mathbf{e}_k|j^+, z_k^t, \mathbf{Z}^{k-1}). \end{aligned} \tag{61}$$

Rearranging and multiplying and dividing by $p(z_k^f|j^+, z_k^t, \mathbf{Z}^{k-1})$ we obtain

$$\begin{aligned} p\left(\mathbf{e}_k|z_k^f, z_k^t, \mathbf{Z}^{k-1}\right) &= \sum_{j^+=1}^{J_k} \frac{\xi_k^t(j^+)}{p\left(z_k^f|z_k^t, \mathbf{Z}^{k-1}\right)} \\ &\quad \times p\left(z_k^f|\mathbf{e}_k\right) p\left(\mathbf{e}_k|j^+, z_k^t, \mathbf{Z}^{k-1}\right) \\ &\quad \times \frac{p\left(z_k^f|j^+, z_k^t, \mathbf{Z}^{k-1}\right)}{p\left(z_k^f|j^+, z_k^t, \mathbf{Z}^{k-1}\right)} \\ &= \sum_{j^+=1}^{J_k} \frac{\xi_k^t(j^+) p\left(z_k^f|j^+, z_k^t, \mathbf{Z}^{k-1}\right)}{p\left(z_k^f|z_k^t, \mathbf{Z}^{k-1}\right)} \\ &\quad \times \frac{p\left(z_k^f|\mathbf{e}_k\right) p\left(\mathbf{e}_k|j^+, z_k^t, \mathbf{Z}^{k-1}\right)}{p\left(z_k^f|j^+, z_k^t, \mathbf{Z}^{k-1}\right)} \end{aligned} \tag{62}$$

which becomes

$$\begin{aligned} p(\mathbf{e}_k|\mathbf{Z}^k) &\triangleq p(\mathbf{e}_k|z_k^f, z_k^t, \mathbf{Z}^{k-1}) \\ &= \sum_{j^+=1}^{J_k} \xi_k(j^+) p(\mathbf{e}_k|j^+, z_k^f, z_k^t, \mathbf{Z}^{k-1}). \end{aligned} \tag{63}$$

The z_k^f measurement is applied to each track component j^+ separately to correct its relative probability, the mean value, and the covariance. The FDOA measurement (10) is nonlinear, and we use extended Kalman filters. Each component remains approximately Gaussian

$$\begin{aligned} p(\mathbf{e}_k|j^+, \mathbf{Z}^k) &\triangleq p\left(\mathbf{e}_k|j^+, z_k^f, z_k^t, \mathbf{Z}^{k-1}\right) \\ &\approx \mathcal{N}\left(\mathbf{e}_k; \hat{\mathbf{e}}_{k|k}(j^+), \mathbf{P}_{k|k}(j^+)\right) \end{aligned} \tag{64}$$

where $\hat{\mathbf{e}}_{k|k}(j^+)$ and $\mathbf{P}_{k|k}(j^+)$ are the posterior mean and covariance of component j^+ respectively.

For reasons of clarity we repeat (10) as

$$z_k^f = h^f(\mathbf{e}_k) + u_k^f. \tag{65}$$

The FDOA EKF update is

$$\begin{aligned} \hat{\mathbf{e}}_{k|k}(j^+) &= \hat{\mathbf{e}}_{k|k}^t(j^+) + \mathbf{K}_k^f(j^+)(z_k^f - h^f(\hat{\mathbf{e}}_{k|k}^t(j^+))) \\ \mathbf{P}_{k|k}(j^+) &= \left(\mathbf{I} - \mathbf{K}_k^f(j^+)\mathbf{H}_k^f(j^+)\right) \mathbf{P}_{k|k}^t(j^+). \end{aligned} \tag{66}$$

The FDOA Kalman gain is

$$\mathbf{K}_k^f(j^+) = \mathbf{P}_{k|k}^t(j^+)\mathbf{H}_k^f(j^+)^\top S_k^f(j^+)^{-1} \tag{67}$$

$$S_k^f(j^+) = \mathbf{H}_k^f(j^+)\mathbf{P}_{k|k}^t(j^+)\mathbf{H}_k^f(j^+)^\top + \sigma_f^2. \tag{68}$$

Define the Jacobian of measurement function $h^f(\mathbf{e})$ as

$$\mathbf{H}^f(\mathbf{e}) \triangleq \frac{\partial h^f(\mathbf{e})}{\partial \mathbf{e}}. \tag{69}$$

Then the FDOA Jacobian for track component j^+ is

$$\mathbf{H}_k^f(j^+) = \mathbf{H}^f(\hat{\mathbf{e}}_{k|k}^t(j^+)). \tag{70}$$

The Jacobian of the FDOA measurement equation is

$$\mathbf{H}^f(\mathbf{e}) = -\frac{f_0}{c} \begin{bmatrix} \mathbf{A}^{(1)} - \mathbf{A}^{(2)} \\ \mathbf{i}^{(1)} - \mathbf{i}^{(2)} \end{bmatrix}^\top \tag{71}$$

where $\mathbf{i}^{(i)}$ is the unit vector from sensor i to the emitter position $\mathbf{e}$ (6), and

$$\mathbf{A}^{(i)} = \mathbf{i}_c^{(i)} \mathbf{i}_c^{(i)^\top} \frac{\left(\dot{\mathbf{x}} - \dot{\mathbf{x}}^{(i)}\right)}{\|\mathbf{r}^{(i)}\|} \tag{72}$$

where $\mathbf{i}_c^{(i)}$ is the unit vector $\mathbf{i}^{(i)}$ rotated by $\pi/2$, i.e.,

$$\mathbf{i}^{(i)} = \begin{bmatrix} \cos(\alpha^{(i)}) \\ \sin(\alpha^{(i)}) \end{bmatrix} \Rightarrow \mathbf{i}_c^{(i)} = \begin{bmatrix} -\sin(\alpha^{(i)}) \\ \cos(\alpha^{(i)}) \end{bmatrix}. \tag{73}$$

A posteriori track component probabilities are (62), (63)

$$\xi_k(j^+) = \frac{\xi_k^t(j^+) p(z_k^f|j^+, z_k^t, \mathbf{Z}^{k-1})}{p(z_k^f|z_k^t, \mathbf{Z}^{k-1})} \tag{74}$$

where FDOA measurement likelihood is given by

$$\begin{aligned} p(z_k^f|z_k^t, \mathbf{Z}^{k-1}) &= \int_{\mathbf{e}_k} p\left(z_k^f|\mathbf{e}_k\right) p\left(\mathbf{e}_k|z_k^t, \mathbf{Z}^{k-1}\right) \mathrm{d}\mathbf{e}_k \\ &= \sum_{j^+=1}^{J_k} \xi_k^t(j^+) p\left(z_k^f|j^+, z_k^t, \mathbf{Z}^{k-1}\right) \end{aligned} \tag{75}$$

and where $p(z_k^f|j^+, z_k^t, \mathbf{Z}^{k-1})$ is calculated by

$$\begin{aligned} p\left(z_k^f|j^+, z_k^t, \mathbf{Z}^{k-1}\right) &= \int_{\mathbf{e}_k} p\left(z_k^f|\mathbf{e}_k\right) p\left(\mathbf{e}_k|j^+, z_k^t, \mathbf{Z}^{k-1}\right) \mathrm{d}\mathbf{e}_k \\ &= \int_{\mathbf{e}_k} \mathcal{N}\left(z_k^f; h^f(\mathbf{e}_k), \sigma_f^2\right) \\ &\quad \times \mathcal{N}\left(\mathbf{e}_k; \hat{\mathbf{e}}_{k|k}^t(j^+), \mathbf{P}_{k|k}^t(j^+)\right) \mathrm{d}\mathbf{e}_k \end{aligned} \tag{76}$$

which simplifies to

$$p(z_k^f|j^+, z_k^t, \mathbf{Z}^{k-1}) \approx \mathcal{N}\left(z_k^f; h^f(\hat{\mathbf{e}}_{k|k}^t(j^+)), S_k^f(j^+)\right) \quad (77)$$

with $S_k^f(j^+)$ defined by (68). From (74)–(77) we have

$$\xi_k(j^+) = \frac{\xi_k^t(j^+)\mathcal{N}\left(z_k^f; h^f(\hat{\mathbf{e}}_{k|k}^t(j^+)), S_k^f(j^+)\right)}{\sum_{j^+}\xi_k^t(j^+)\mathcal{N}\left(z_k^f; h^f(\hat{\mathbf{e}}_{k|k}^t(j^+)), S_k^f(j^+)\right)}. \quad (78)$$

E. Track Outputs

Output state estimate mean and covariance are the mean and the covariance of track state Gaussian mixture respectively

$$\begin{aligned}\hat{\mathbf{e}}_{k|k} &= \sum_{j^+=1}^{J_k}\xi_k(j^+)\hat{\mathbf{e}}_{k|k}(j^+)\\ \mathbf{P}_{k|k} &= \sum_{j^+=1}^{J_k}\xi_k(j^+)\left(\mathbf{P}_{k|k}(j^+) + \hat{\mathbf{e}}_{k|k}(j^+)\hat{\mathbf{e}}_{k|k}(j^+)^\top\right)\\ &\quad - \hat{\mathbf{e}}_{k|k}\hat{\mathbf{e}}_{k|k}^\top. \end{aligned} \quad (79)$$

F. Track Component Management

The measurement update at time k increases the number of track components by factor G_k. Left unchecked, the number of track components increases exponentially in time.

Although not formally part of the algorithm itself, any practical implementation must limit the number of track components at the end of every measurement update cycle. The internal structure of proposed filter corresponds to the integrated track splitting filter [24] and multihypothesis tracking [25]. Thus all track component control techniques described for MHT and ITS may be implemented here.

Available techniques include the track component pruning and the component subtree removing (removing track components with low probability) [26], as well as the track component merging. The track component merging merges track components with similar state into one track component. Various criteria for selecting track components to merge are available [27], [28].

In the simulation study, the authors implement the track component merge method proposed in [29] together with the track component pruning. [29] proposes merging of all track components with common measurement sequence in the last number of updates (in our case two).

G. Track Initialization

The track is initialized using the first measurement pair $\mathbf{z}_1 = \{z_1^t, z_1^f\}$. We first apply the TDOA measurement z_1^t, followed by the FDOA measurement z_1^f.

Each component g of the GMM representation of the TDOA measurement $\mathbf{z}_1^t$ translates into one component j^+ of new track. The position components (x and y Cartesian components) of $\hat{\mathbf{e}}_{1|1}^t(j^+)$ and $\mathbf{P}_{1|1}^t(j^+)$ are equal to $\mathbf{w}_1^t(j^+)$ and $\mathbf{R}_1^t(j^+), j^+ = 1\cdots G_1$, respectively. The velocity components of $\hat{\mathbf{e}}_{1|1}^t(j^+)$ are equal to zero. The velocity components of $\mathbf{P}_{1|1}^t(j^+)$ are equal to $V_{\max}^2\mathbf{I}_2/3$, where $V_{\max}$ denotes the maximum emitter speed. The FDOA measurement z_1^f is then applied as described in Section IV-D, followed by the track component management.

V. Algorithm Benchmarks

Results of proposed GMM-ITS-based filter are compared with an EKF-based solution, as well as with the Cramér–Rao lower bounds of rms estimation errors.

A. Extended Kalman Filter Bank

The EKF is an industry standard solution for nonlinear estimation. The EKF here linearizes measurement equation in the vicinity of the predicted emitter position. It requires a good initial guess to start target tracking [16]. To help in this respect, a bank of filters is initialized and updated, and we use the acronym EKFb.

Each filter is termed a track component. Each track component approximates track state by a Gaussian pdf with its relative probability. The EKFb track state pdf is a Gaussian mixture, described in Section IV-A, (40). The EKFb track prediction is described in Section IV-B. Each track component is updated by the TDOA measurement z_k^t and then by the FDOA measurement z_k^f. Each measurement uses the corresponding EKF. The FDOA EKF is also used in the GMM-ITS update, and is already described in Section IV-D. Here we describe the TDOA EKF update and the update of the track component relative probabilities. Please note that only existing track components are updated, i.e., new components are not being created and $j^+ = j$. The EKFb is a static bank of filters, as opposed to the GMM-ITS which is a dynamic bank of filters.

For reasons of clarity we repeat (5) as

$$z_k^t = h^t(\mathbf{e}_k) + u_k^t. \quad (80)$$

The TDOA EKF update of the track component j is

$$\begin{aligned}\hat{\mathbf{e}}_{k|k}^t(j) &= \hat{\mathbf{e}}_{k\,|\,k-1}(j) + \mathbf{K}_k^t(j)\left(z_k^t - h^t(\hat{\mathbf{e}}_{k\,|\,k-1}(j))\right)\\ \mathbf{P}_{k|k}^t(j) &= \left(\mathbf{I} - \mathbf{K}_k^t(j)\mathbf{H}_k^t(j)\right)\mathbf{P}_{k\,|\,k-1}(j).\end{aligned} \quad (81)$$

The TDOA Kalman gain is

$$\mathbf{K}_k^t(j) = \mathbf{P}_{k\,|\,k-1}(j)\mathbf{H}_k^t(j)^\top S_k^t(j)^{-1} \quad (82)$$

$$S_k^t(j) = \mathbf{H}_k^t(j)\mathbf{P}_{k\,|\,k-1}(j)\mathbf{H}_k^t(j)^\top + \sigma_t^2. \quad (83)$$

Define the Jacobian of measurement function $h^t(\mathbf{e})$ as

$$\mathbf{H}^t(\mathbf{e}) \triangleq \frac{\partial h^t(\mathbf{e})}{\partial \mathbf{e}}. \quad (84)$$

Then the track component j TDOA measurement matrix is

$$\mathbf{H}_k^t(j) = \mathbf{H}^t(\hat{\mathbf{e}}_{k\,|\,k-1}(j)). \quad (85)$$

It is straightforward to derive

$$\mathbf{H}^t(\mathbf{e}) = \frac{1}{c}\left(\mathbf{i}^{(1)} - \mathbf{i}^{(2)}\right)^\top \mathbf{H} \quad (86)$$

where $\mathbf{i}^{(i)}$ is the unit vector from sensor i to the emitter position $\mathbf{e}$ (6).

The measurement likelihood with respect to the track component j is

$$p(z_k^t, z_k^f|j, \mathbf{Z}^{k-1}) = p(z_k^t|j, \mathbf{Z}^{k-1})p(z_k^f|j, z_k^t, \mathbf{Z}^{k-1}) \quad (87)$$

where the TDOA measurement likelihood is

$$p(z_k^t|j,\mathbf{Z}^{k-1}) \approx \mathcal{N}\left(z_k^t; h^t(\hat{\mathbf{e}}_{k\,|\,k-1}(j)), S_k^t(j)\right) \tag{88}$$

and the FDOA measurement likelihood is (77)

$$p(z_k^f|j,z_k^t,\mathbf{Z}^{k-1}) \approx \mathcal{N}\left(z_k^f; h^f(\hat{\mathbf{e}}_{k|k}^t(j)), S_k^f(j)\right). \tag{89}$$

Updated relative track component probabilities are

$$\xi_k(j) = \frac{\xi_{k-1}(j)p(z_k^t,z_k^f|j,\mathbf{Z}^{k-1})}{p(z_k^t,z_k^f|\mathbf{Z}^{k-1})}. \tag{90}$$

Using (87)–(90) we derive (91), shown at the bottom of the page.

The number of track components in the EKFb never increases, and there is little need for component management. However, one may delete (terminate) track components with very low relative probability, to further decrease average computational requirements. The EKFb track outputs are the mean and the covariance of state estimate pdf, as described in Section IV-E and (79).

The EKFb is initialized in the manner described in Section IV-G. Track state pdf after the first pair of TDOA and FDOA measurements is identical for both GMM-ITS and EKFb.

B. Cramér–Rao Lower Bounds

The CRLB determines the best achievable second-order error performance

$$\mathbb{E}\left\{(\mathbf{e}_k - \hat{\mathbf{e}}_{k|k})(\mathbf{e}_k - \hat{\mathbf{e}}_{k|k})^\top\right\} \geq \mathbf{J}_k^{-1} \tag{92}$$

where $\geq$ is defined as

$$\mathbf{G}_1 \geq \mathbf{G}_2 \Rightarrow \mathbf{G}_1 - \mathbf{G}_2 \geq 0 \tag{93}$$

i.e., $\mathbf{G}_1 - \mathbf{G}_2$ is positive semidefinite. $\mathbf{J}_k$ denotes the Fisher information matrix at time k.

The lower bound of rms estimation position error is

$$\sigma_k^p = \sqrt{\mathrm{tr}\left(\mathbf{H}\mathbf{J}_{\mathrm{k}}^{-1}\mathbf{H}^\top\right)} \tag{94}$$

where tr denotes the square matrix trace operation.

Assuming, as we do in the simulation experiments, zero emitter trajectory plant noise covariance, $\mathbf{Q}_k = \mathbf{0}$, the FIM at time k equals [30], [31]

$$\mathbf{J}_k = \left[\mathbf{F}_k^{-1}\right]^\top \mathbf{J}_{k-1}\left[\mathbf{F}_k^{-1}\right] + \frac{1}{\sigma_t^2}\mathbf{H}^t(\mathbf{e}_k)^\top\mathbf{H}^t(\mathbf{e}_k) + \frac{1}{\sigma_f^2}\mathbf{H}^f(\mathbf{e}_k)^\top\mathbf{H}^f(\mathbf{e}_k) \tag{95}$$

where $\mathbf{F}_k$ is the emitter trajectory propagation matrix, and the TDOA and FDOA measurement matrices, $\mathbf{H}^t(\mathbf{e}_k)$ and $\mathbf{H}^f(\mathbf{e}_k)$ are evaluated at true emitter trajectory state, and are defined by (86) and (71) respectively.

The recursion $\mathbf{J}_0$ is initialized by prior information. It includes the size of the surveillance area, as well as the maximum emitter velocity, as proposed in [31].

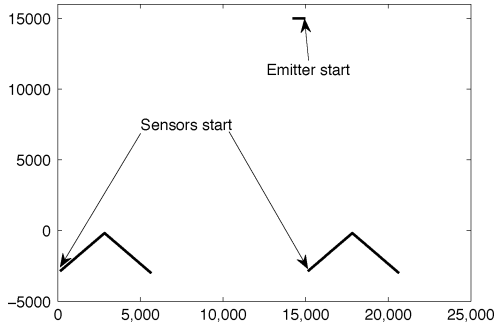

Fig. 5. Mobile emitter geolocation scenario.

VI. Simulation Experiments

Here we consider geolocation of a mobile emitter. We compare the following:

- GMM-ITS filter using only TDOA measurements (curves labeled "TDOA");
- GMM-ITS filter, as proposed in this paper (curves labeled "TFDOA");
- EKFb filter bank as described in Section V-A (curves labeled "EKFb");
- Cramér–Rao lower bounds, as presented in Section V-B (curves labeled "CRLB").

As can be seen in Fig. 1, the TDOA measurements are akin to the bearings only measurements. The assumption is that the single emitter moves with uniform motion (constant velocity), and that the sensors perform maneuvers to ensure observability. The simulated scenario is depicted in Fig. 5. The sensors move with a constant speed (but not constant velocity) of 100 m/s. Each simulation run simulates 80 s, and the simulation statistics are accumulated over 1000 runs.

In all experiments it is observed that the estimation errors decrease significantly immediately after the sensor maneuver is performed at the 40-s instant. The maximum emitter speed constraint is set to $V_{\max} = 15$ m/s. Three sets of emitter movements have been simulated:

- stationary emitter;
- constant emitter speed in the x-direction of -10 m/s, as shown in Fig. 5;
- constant emitter speed in the y-direction of -10 m/s.

For all filters results were similar, however the biggest estimation errors were recorded in the second case, which is presented here. The TDOA and the FDOA measurements are created by adding samples of zero mean mutually independent white

$$\xi_k(j) = \frac{\xi_{k-1}(j)\mathcal{N}\left(z_k^t; h^t(\hat{\mathbf{e}}_{k\,|\,k-1}(j)), S_k^t(j)\right)\mathcal{N}\left(z_k^f; h^f(\hat{\mathbf{e}}_{k|k}^t(j)), S_k^f(j)\right)}{\sum_j \xi_{k-1}(j)\mathcal{N}\left(z_k^t; h^t(\hat{\mathbf{e}}_{k\,|\,k-1}(j)), S_k^t(j)\right)\mathcal{N}\left(z_k^f; h^f(\hat{\mathbf{e}}_{k|k}^t(j)), S_k^f(j)\right)} \tag{91}$$

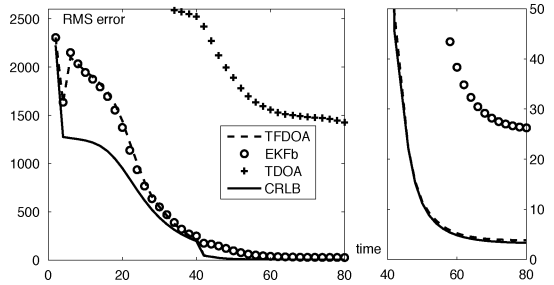

Fig. 6. Minimal measurement errors—output rms errors.

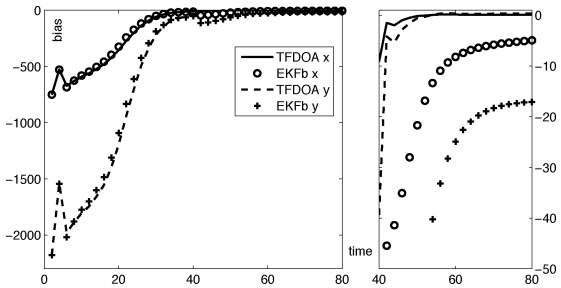

Fig. 7. Minimal measurement errors—output bias.

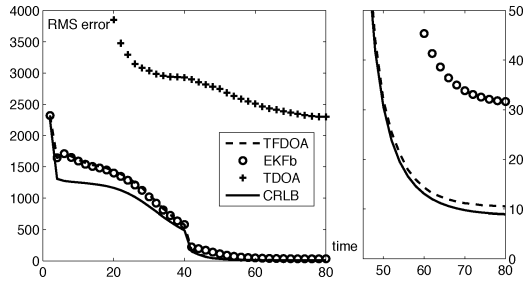

Fig. 8. Increased measurement errors—output rms errors.

Gaussian errors to the true TDOA and FDOA values. Emitter signal is assumed to be the narrow band communication signal outlined in Section II-C. The measurements are returned simultaneously every $2s$. Minimal TDOA and FDOA measurement errors standard deviations are $30/c$ [m], and $3.7f_0/c$ [mm/s] respectively, as per (11). To allow for additional, equipment induced errors, we also consider increased TDOA and FDOA measurement errors having standard deviations of $100/c$ [m], and $10f_0/c$ [mm/s] respectively.

The position rms estimation errors and estimation bias for the case of minimal TDOA and FDOA measurement errors are presented in Figs. 6 and 7 respectively. The position rms estimation errors and estimation bias for the case of increased TDOA and FDOA measurement errors are presented in Figs. 8 and 9 respectively. Each figure also "zooms in" the period after the sensor maneuvers, when the observability increases, and estimation errors decrease significantly. This is the period of useful results, and of most interest.

A general conclusion is that in this scenario the "TDOA" results are not useful, due to large estimation errors. The "EKFb" results are significantly better. However the "TFDOA" results further significantly decrease estimation errors. Furthermore, the performance of "TFDOA" nears the theoretical optimum of

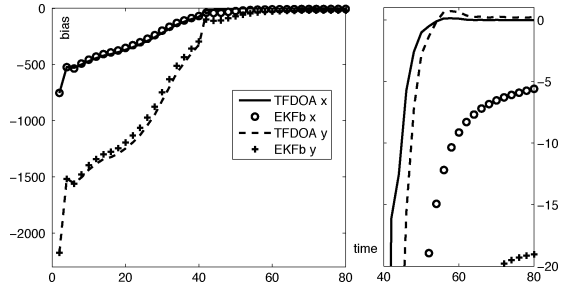

Fig. 9. Increased measurement errors—output bias.

the "CRLB" curve, at least in the "zoomed in" area of interest. The final "TFDOA" rms estimation errors of 3.8 and 10.5 m for the case of minimal and increased measurement errors respectively in this scenario (with the emitter more than 15 km away) is certainly a useful outcome.

Choosing the number of measurement components, and the maximum number of track components is a tradeoff between computational requirements and the estimator performance. In our simulations, the number G_k of TDOA measurement components was 60, and the number of track components was limited to 40. However, as the components with relative probabilities less than 10^{-3} were pruned, the number of actual track components J_k varied between 20 and 40.

Each simulation experiment consists of 1000 simulation runs, each providing 40 pairs of TDOA and FDOA measurements. Each simulation experiments consists of 40 000 filter updates. Execution times for the "EKFb" simulation experiments were 270 and 340 s for the minimal and increased measurement errors. This corresponds to 6.8 and 8.5 ms respectively per filter update. The "TFDOA" corresponding execution times were 1600 and 2300 s, which corresponds to 40 and 58 ms per filter update respectively. This fits comfortably within the real-time requirements of 2 s per filter update. The experiments were conducted on a computer with Intel Pentium 1.73-GHz processor, running Matlab under Microsoft Windows. Using faster (digital signal processor) processors, a real-time operating system, and optimized coding would yield further significant reduction in execution times.

VII. Conclusion

This paper presents a mobile emitter geolocaton method based on integrating information from TDOA and FDOA measurements over time. These measurements may be efficiently obtained and are well within current state of the art.

Although the TDOA measurements are nonlinear, emitter position estimation using the TDOA measurement is performed by essentially linear operations, i.e., Kalman filter update. This was accomplished by representing both non-Gaussian state estimate pdf and non-Gaussian TDOA measurement likelihood by respective Gaussian mixtures, as well as using a dynamic bank of Kalman filters in the form of a track splitting filter. Each Kalman filter output has relatively small covariance, which enables efficient emitter position update using FDOA measurement using an EKF filter.

This extension of the GMM-ITS filter is also applicable to other nonlinear problems, where some (but not all) of the measurements available are not amenable to the Gaussian mixture likelihood approximation.

Simulation experiments have shown that proposed filtering can be accomplished in real time with only modest computational resources. Performance of the proposed algorithm, at least in the simulated scenario, significantly improves upon the EKF-based industry standard, and is near theoretical Cramér–Rao bounds.

REFERENCES

[1] M. Schmidt, "A new approach to geometry of range difference location," *IEEE Trans. Aerosp. Electron. Syst.*, vol. 8, no. 6, pp. 821–835, Nov. 1972.

[2] K. Ho and Y. Chan, "Solution and performance analysis of geolocation by TDOA," *IEEE Trans. Aerosp. Electron. Syst.*, vol. 29, no. 4, pp. 1311–1322, Oct. 1993.

[3] F. Fletcher, B. Ristic, and D. Mušicki, "TDOA measurements from two UAVs," in *10th Int. Conf. Inf. Fusion, Fusion 2007*, Quebec, QC, Canada, Jul. 2007.

[4] S. Stein, "Algorithms for ambiguity function processing," *IEEE Trans. Acoust., Speech Signal Process.*, vol. ASSP-29, no. 3, pp. 588–599, Jun. 1981.

[5] S. Stein, "Differential delay/Doppler ML estimation with unknown signals," *IEEE Trans. Signal Process.*, vol. 41, no. 8, pp. 2717–2719, Aug. 1993.

[6] H. Wax, "The joint estimation of differential delay, doppler and phase," *IEEE Trans. Inf. Theory*, vol. IT-28, no. 5, pp. 817–820, Sep. 1982.

[7] E. Weinstein and D. Kletter, "Delay and doppler estimation by time-space partition of the array data," *IEEE Trans. Acoust., Speech Signal Process.*, vol. ASSP-31, no. 6, pp. 1523–1535, Dec. 1983.

[8] B. Friedlander, "On the Cramer-Rao bound for time delay and Doppler estimation," *IEEE Trans. Inf. Theory*, vol. IT-28, no. 3, pp. 575–580, May 1984.

[9] R. Bardelli, D. Haworth, and N. Smith, "Interference localization for the eutelsat satellite system," in *Global Telecommun. Conf., GLOBECOM'95*, , Singapore, Nov. 1995, vol. 3, pp. 1641–1651.

[10] P. Chestnut, "Emitter localization accuracy using TDOA and differential doppler," *IEEE Trans. Aerosp. Electron. Syst.*, vol. AES-18, no. 2, pp. 214–218, Mar. 1982.

[11] M. Chen and M. L. Fowler, "Geometry-adaptive data compression for TDOA/FDOA location [wireless sensor network applications]," in *2005 IEEE Int. Conf. Acoust., Speech Signal Process.*, Philadelphia, PA, Mar. 2005.

[12] H. Wei, C. Xia, and S. Ye, "Motion detection using Rao test in dual-satellite geolocation system," in *8th Int. Conf. Signal Process.*, Beijing, China, Nov. 2006.

[13] G. Yao, Z. Liu, and Y. Xu, "TDOA/FDOA joint estimation in a correlated noise environment," in *IEEE Int. Symp. Microwave, Antenna, Propagation EMC Technol. Wireless Commun.*, Beijing, China, Aug. 2005.

[14] K. C. Ho, X. Lu, and L. Kovavisaruch, "Source localization using TDOA and FDOA measurements in the presence of receiver location errors: Analysis and solution," *IEEE Trans. Signal Process.*, vol. 55, no. 2, pp. 684–696, Feb. 2007.

[15] K. C. Ho and Y. T. Chan, "Geolocation of a known altitude object from TDOA and FDOA measurements," *IEEE Trans. Aerosp. Electron. Syst.*, vol. AES-18, no. 2, pp. 214–218, Mar. 1982.

[16] K. C. Ho and W. Xu, "An accurate algebraic solution for moving source location using TDOA and FDOA measurements," *IEEE Trans. Signal Process.*, vol. 52, no. 9, pp. 2453–2463, Sep. 2004.

[17] R. Stansfield, "Statistical theory of DF fixing," *J. IEE*, vol. 94, no. 15, pp. 762–770, 1947.

[18] K. Becker, "Three-dimensional target motion analysis using angle and frequency measurements," *IEEE Trans. Aerosp. Electron. Syst.*, vol. 41, no. 1, pp. 284–301, Jan. 2005.

[19] K. Becker, "An efficient method of passive emitter location," *IEEE Trans. Aerosp. Electron. Syst.*, vol. 28, no. 4, pp. 1091–1104, Oct. 1992.

[20] J. Kaufmann and W. Hutchinson, Emitter location with LES-9/9 using differential time of arrival and differential Doppler shift Lincoln Lab., MIT, Lexington, MA, Rep. 698 (Rev. 1), 2000.

[21] D. Mušicki and R. Evans, "Measurement Gaussian sum mixture target tracking," in *9th Int. Conf. Inf. Fusion*, Florence, Italy, Jul. 2006.

[22] D. Mušicki and W. Koch, "Geolocation using TDOA and FDOA measurements," in *11th Int. Conf. Inf. Fusion*, Cologne, Germany, Jun./Jul. 2008.

[23] D. L. Alspach and H. W. Sorenson, "Nonlinear Bayesian estimation using Gaussian sum approximation," *IEEE Trans. Automatic Contr.*, vol. 17, no. 4, pp. 439–448, Apr. 1972.

[24] D. Mušicki, B. La Scala, and R. Evans, "The integrated track splitting filter—Efficient multi-scan single target tracking in clutter," *IEEE Trans. Aerospace Electron. Syst.*, vol. 43, no. 4, pp. 1409–1425, Oct. 2007.

[25] S. Blackman, *Multiple-Target Tracking With Radar Applications*. Norwood, MA: Artech House, 1986.

[26] S. Blackman and R. Popoli, *Design and Analysis of Modern Tracking Systems*. Norwood, MA: Artech House, 1999.

[27] D. J. Salmond, "Mixture reduction algorithms for target tracking in clutter," in *Proc. SPIE: Signal and Data Processing of Small Targets*, Orlando, FL, Apr. 1990, vol. 1305, pp. 434–445.

[28] J. L. Williams and P. S. Mayback, "Cost-function-based Gaussian mixture reduction for target tracking," in *5th Int. Conf. Inf. Fusion, Fusion 2003*, Cairns, Queensland, Australia, Jul. 2003, pp. 1047–1054.

[29] R. A. Singer, R. G. Sea, and K. B. Housewright, "Derivation and evaluation of improved tracking filters for use in dense multi-target environments," *IEEE Trans. Inf. Theory*, vol. IT-20, no. 4, pp. 423–432, Jul. 1974.

[30] P. Tichavsky, C. H. Muravchik, and A. Nehorai, "Posterior Cramèr Rao bounds for discrete time nonlinear filtering," *IEEE Trans. Signal Process.*, vol. 46, no. 5, pp. 1386–1396, May 1998.

[31] B. Ristic, S. Arulampalam, and N. Gordon, *Beyond the Kalman Filter*. Norwood, MA: Artech House, 2004.

Darko Mušicki (M'90) was born in Belgrade, Serbia, in 1957. He received the B.E. degree in electrical engineering and the M.Sc. degree in communications from the University of Belgrade, in 1979 and 1984, respectively, and the Ph.D. degree from the University of Newcastle, NSW, Newcastle, Australia, in 1994.

After he received the B.E. degree, he worked in the area of radar system design and simulations, as well as fast implementation of digital signal processing algorithms. He was member of academic staff at the University of Belgrade between 1985 and 1988. He moved to Australia in 1988. He was working for Entropy Data Pty Ltd from 1988–2002, when he joined the University of Melbourne, Australia. He is now with the Department of Electronic Information Systems Engineering, Hanyang University, Kyunggido, Korea. Since 1984 he has been involved in target-tracking research and design, sensor information fusion, and nonlinear estimation, as well as resource allocation and wireless sensor networks. He is the author/coauthor of a number of often-cited publications in his chosen fields.

Dr. Mušicki is member of Board of Directors of the International Society for Information Fusion (ISIF), and has served as ISIF President during 2008.

Regina Kaune received the university degree in mathematics and chemistry from the University of Cologne, Cologne, Germany, in 2007.

Since 2008 she has been working in the Sensor Networks and Data Fusion Department, Fraunhofer Institute for Communication Information Processing and Ergonomics FKIE, Wachtberg, Germany. Her current research interests include passive target tracking and estimation theory.

Wolfgang Koch (M'97–SM'09) studied mathematics and physics and received the Ph.D. degree from the Aachen Technical University, Aachen, Germany, in 1990.

At present he is Head of the Sensor Data and Information Fusion (SDF) Department, Fraunhofer FKIE. His current research interests are related to statistical estimation theory, multiple-data sensor fusion, multiple-target tracking, sensor management, ground surveillance, passive surveillance, multistatic tracking, and sensor data/information fusion in general. On this area, he has published several book chapters and numerous journal and conference papers. At Bonn University, Institute of Computer Science, he regularly gives lectures related to sensor data fusion.

Dr. Koch is a Technical Editor of "Target Tracking and Multisensor Systems" for the IEEE TRANSACTIONS ON AEROSPACE AND ELECTRONIC SYSTEMS. Together with Peter Willett, University of Connecticut (U.S.) he is Co-Chairman of FUSION 2008 in Cologne, Germany.